ACS OMEGA

http://pubs.acs.org/journal/acsodf

Article

Silicone Nanofilament Coatings as Flexible Catalyst Supports for a Knoevenagel Condensation Reaction in Batch and Flow Systems

Yuen-Yee Lau, Kangwei Chen, Shanqiu Liu, Lukas Reith, and Stefan Seeger*

Cite This: *ACS Omega* 2022, 7, 39463−39470

Read Online

ACCESS | Metrics & More | Article Recommendations | Supporting Information

ABSTRACT: In this work, silicone nanofilament (SNF) coatings were prepared via a droplet-assisted growth and shaping (DAGS) approach, where the preparation of the coatings is allowed under ambient conditions. The application of SNF coatings as catalyst supports for amino moieties from (3-aminopropyl)triethoxysilane (APTES) was investigated. With the optimized coating conditions identified, the Brunauer−Emmett−Teller surface areas of a bare glass filter substrate and bare glass beads after the coating have increased by 5-fold and 16-fold, respectively. The SNF-coated filters were readily functionalized with amino groups via a liquid-phase deposition process, and their catalytic activities for a Knoevenagel reaction were evaluated using a batch reactor and a packed bed reactor. In both reactors, the as-prepared filters demonstrated superior catalytic performance over the functionalized filters without SNF coatings. Notably, the unique flexibility of the SNF coatings allowed the facile preparation of a packed bed reactor and a scalable catalytic system. It is expected that the packed bed system established in this study will support the development and the use of various SNF-supported organocatalysts and catalytic materials.

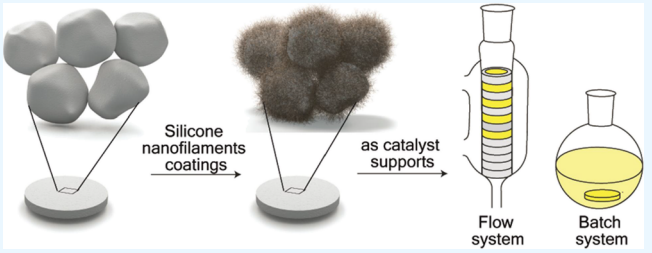

1. INTRODUCTION

During the past years, our group has established a highly facile method to grow silicone-based nanostructures on substrates via a droplet-assisted growth and shaping (DAGS) approach at room temperature.[1,2] Depending on the applied coating conditions, nano- and microstructures in various shapes can be obtained.[2] In the case of nanofilaments, the structures can grow with the lengths of tens of micrometers, forming dense carpets of silicone nanofilaments (SNFs) on the substrates. Substrates coated with SNFs lead to a significant increase in the surface area,[3] exhibited superhydrophobicity due to surface roughness,[1] and demonstrated excellent thermal and chemical stability.[1,3]

To date, there is a significant amount of research interest in utilizing SNFs to develop surfaces with extreme wetting properties, such as superhydrophobic,[4,5] superoleophilic,[6,7] and superamphiphobic surfaces.[8,9] Most of the applications were related to self-cleaning,[5,10,11] antifouling,[12,13] or oil/water separation purposes.[7,8,13−15] Given that numerous materials with fibrous morphologies, such as carbon nanofibers, cellulose nanofibers, and polymeric fibers, are among some of the very promising catalysts supports or catalysts, studies related to the catalytic applications of SNFs are lacking. Nevertheless, SNFs have demonstrated to be some promising high surface area support materials for metal catalysts, including Pt,[16] TiO_2,[17] and nickel oxides.[18] In addition, various organic functionalities have been grafted on the surfaces of SNFs. Li et al.[19] reported a photoinduced approach to introduce thiol and disulfide groups on SNFs. Zimmermann et al.[20] introduced amino and carboxy groups on SNFs for the immobilization of proteins. Chu et al.[21] demonstrated the use of *N*-(3-trimethoxysilylpropyl)-diethylenetriamine to modify an SNF-coated support and utilized it in supporting a Knoevenagel condensation reaction. This urged for more thorough studies on the catalytic applications of these amino-functionalized SNFs.

A major concern with the applications of these SNF-supported catalysts for liquid-phase reactions is the mechanical attrition. As SNFs protrude from surfaces, it can be expected that stirring in a batch reactor can be detrimental to the nanostructures. The implementation of a flow system has been considered a promising strategy to circumvent the attrition problem and allow the ease of separation of the solid catalysts from the reaction mixture.[22] There are generally three types of reactors to carry out heterogeneous catalysis in flow, namely, packed bed, monolithic, and wall-coated reactors.[23] Herein, SNFs were grown on porous glass filters, where the filters were sintered from glass beads of the micrometer range. The as-prepared SNF filters were then organically functionalized and packed as a column reactor. The flow of the system was pressure-driven, where reagents were circulated through the

Received: September 23, 2022
Accepted: October 10, 2022
Published: October 20, 2022

column reactor during the reaction. The establishment of the as-prepared flow reactor has facilitated the use of SNF-supported catalysts and demonstrated adaptability to system scaling.

Notably, SNF coatings have some intriguing advantages when compared to other catalyst support materials. First, the DAGS approach for the synthesis of SNFs is highly facile and relatively sustainable when compared to the typical catalytic chemical vapor deposition (CCVD) processes. CCVD is widely employed for the synthesis of some highly promising catalysts support materials in industries, such as carbon nanotubes,[24] carbon nanofibers,[25] and graphene.[26] On the other hand, the preparation of SNF coatings can be carried out under ambient conditions, either in the gas phase[1] or in the liquid phase.[20] In the case of gas-phase coating, only short-chain silanes and water are required as inputs, with no carrier gas needed and waste solvents generated. The process is also applicable to coat a variety of materials, such as glass, titanium, polyester, and ceramics.[1,27] On the contrary, CCVD is only applicable to substrates with high temperature tolerance.[28] Second, SNF benefits from the versatility as silica-based materials, where the surface silanols allow the ease of grafting various active organic functional groups. In contrast, high temperature is often a prerequisite for the functionalization of the aforementioned carbon materials.[24]

In this study, a range of conditions to optimize the extent of SNF growth on glass substrates and the subsequent loading of the amino functionalities were examined. (3-Aminopropyl)-triethoxysilane (APTES), a widely used silane coupling agent, was employed for surface functionalization. This is to demonstrate the applicability of SNFs to be used as a convenient support for grafting organocatalysts. Because of the limitations in using classical methods to quantify the amine content of the thin layer of SNF coatings were observed, a quantification method based on the principle of acid−base titration was adopted and verified. Finally, the catalytic performance of the amino-functionalized SNF composites with the use of a batch reactor and the newly developed packed bed reactor was investigated.

2. EXPERIMENTAL SECTION

2.1. Materials and Instrumentation. Silicone nanofilament (SNF) coatings were performed on sintered glass filter discs (disc diameter = 20 mm, disc height = 3 mm, porosity 3 equivalent to pore size range = 16−40 μm) from Duran, glass beads (size range = 90−150 μm) were from Microbeads AG, Switzerland, and microscope slides (dimensions 76 mm × 26 mm × 1 mm) were from Menzel. Ethyltrichlorosilane (ETCS, 98%) was from ABCR, Germany. (3-Aminopropyl)-triethoxysilane (APTES, 99%), 4-hydroxybenzaldehyde (98%), ethyl cyanoacetate (≥98%), hexane (HPLC grade, ≥97%), and duroquinone (97%) were from Sigma-Aldrich and were used as received. Ethanol absolute (≥99.8%) was from VWR Chemicals. 3-Aminopropyl-functionalized silica gel (40−63 μm, ∼1 mmol/g NH_2 loading) was purchased from Sigma-Aldrich and was used as the control sample for APTES characterization. Brunauer−Emmett−Teller (BET) measurements were carried out with a Quantachrome Quadrasorb SI porosimeter with the use of nitrogen as the adsorption/desorption gas at 77 K. Prior to measurement, samples were degassed at no less than 80 °C for 40 h under vacuum. The BET surface areas were then calculated using the multipoint model with relative pressures (P/P0) in the range of 0.05−0.3 applied. Scanning electron microscopy (SEM) images were recorded using a Zeiss Supra 50 VP at 5 kV, and samples were sputter-coated with 15 nm platinum. Proton nuclear magnetic resonance (^{1}H NMR) was performed on a Bruker AV2−400 spectrometer at 400 MHz using $CDCl_3$ as the solvent. The spectra obtained were used to determine the conversion of the reactants. Duroquinone was added to the NMR samples as an internal standard to calculate the reaction conversions. Attenuated total reflection-Fourier transform infrared (ATR-FTIR) spectra were acquired on a Bruker Vertex 70 with a single reflection diamond ATR accessory. Spectra were recorded over the range of 600−4000 cm^{-1} at a resolution of 2 cm^{-1}.

2.2. SNF Coating (Filter-SNF). Glass filter discs were pretreated with ultrasound in 1 M KOH aqueous solution, rinsed with deionized water, and dried in an oven at 50 °C overnight. Prior to coating, filters were treated with oxygen plasma using a Femto plasma machine (Diener Electronics GmbH & Co. KG, Germany) for 30 min using an oxygen pressure of 0.6 bar, a generator power of 100 W, and a volumetric flow rate of 2 standard cubic centimeter per minute (sccm). The coating was conducted in the gas phase using a glass desiccator (DN100, Duran) as the coating chamber. Two activated filters were fixed in a polytetrafluoroethylene (PTFE) holder and placed inside the chamber. The coating chamber was flushed with a mixture of dry and wet nitrogen at 27.0 ± 0.5 °C and 35 ± 5% relative humidity (rh) for 2 h to pre-equilibrate the system. The temperature and relative humidity of the nitrogen stream were monitored using a hygrometer (EE23, E + E Elektronik). The reaction was started by the injection of 1.5 mL of ethyltrichlorosilane (ETCS) through a septum into a PTFE container placed inside the chamber, and the filters were left for 16 h incubation. To end the reaction, the filters were flushed with nitrogen for 30 min before removing from the chamber. For filters being used in the BET measurement, the temperature of the coating chamber was adjusted to two different temperatures: 23 and 27 °C during the pre-equilibration through nitrogen flushing. Furthermore, filters were pre-equilibrated for 3 h and left for at least 20 h incubation to maximize the SNF gains. The corresponding BET values of the SNF-coated filters were recorded. For glass beads being used in the BET measurement, 2 g of glass beads was activated with oxygen plasma for 30 min with a generator power of 100 W. The coating procedures were the same as described for filters, and the BET value of glass beads pre-equilibrated at 23 °C was recorded.

2.3. APTES Functionalization and Characterization (Filter-SNF-AP). Filters with SNF coatings were treated with oxygen plasma with a low flow rate (100 W, 60 min, 2 sccm). The activated filters were immersed in 20 mL of hexane with 250 μL of APTES added (∼50 mM APTES). The solution was stirred in a custom-made vessel for 16 h at room temperature, where the stirrer did not touch the filter. Afterward, the modified filters (Filter-SNF-AP) were rinsed with hexane, ethanol absolute, and dried in an oven at 80 °C for 4 h. The extent of APTES modification was determined based on an acid exchange capacity method described in the literature.[29] A Filter-SNF-AP was immersed into 100 mL of 1 mM HCl for 1 h at room temperature. Five replicates were performed. The amount of accessible amino groups grafted was calculated from the amount of acid consumed. A pH meter (Seven2Go, Mettler Toledo) was used to serve the purpose. The modified method was validated using a commercial silica gel product

https://doi.org/10.1021/acsomega.2c06157
ACS Omega 2022, 7, 39463−39470

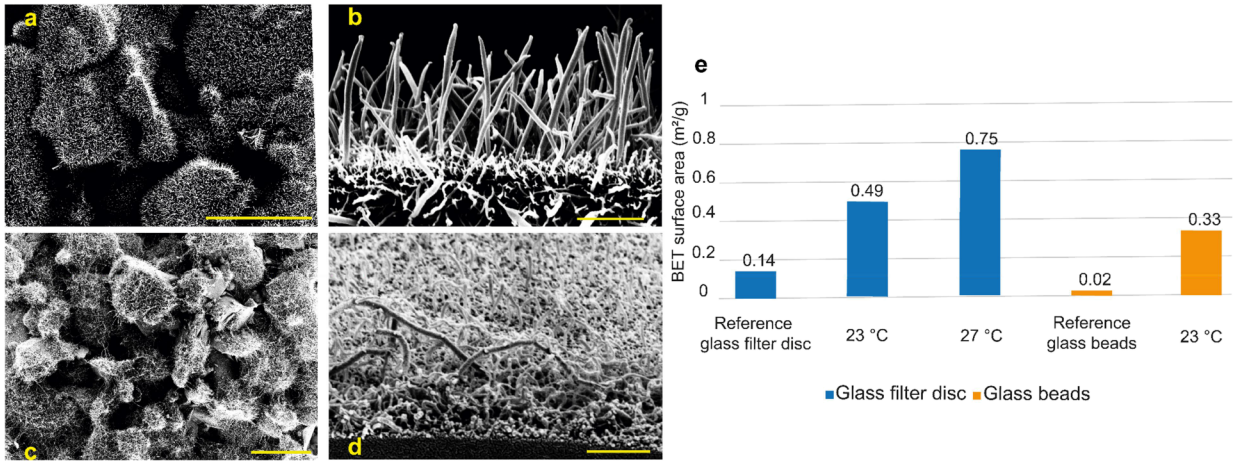

Figure 1. SEM images of filters incubated in a chamber with a continuous supply of humidified nitrogen flow at 27 °C and 35% rh throughout the 16 h coating. (a) Top view, scale bar corresponds to 50 μm. (b) Side view, scale bar corresponds to 2 μm. SEM images of filters pre-equilibrated with humidified nitrogen flow at 23 °C and 35% rh for 2 h prior to coating. (c) Top view, scale bar corresponds to 100 μm. (d) Side view, scale bar corresponds to 1 μm. (e) Comparison of the BET surface area between substrates before and after the SNF coating. Filters pre-equilibrated at 23 and 27 °C were measured, whereas glass beads pre-equilibrated at 23 °C were measured.

with a known amount of grafted 3-aminopropyl functional groups. Silica gels (23 mg) were immersed into 30 mL of 1 mM HCl for 1 h at room temperature. Five replicates were performed. ATR-FTIR spectra were acquired of SNFs in their freestanding forms. Microscope slides were coated with the SNF according to a published protocol[1] and functionalized with the same procedures as filters. Both the SNF and functionalized SNF were scratched off from microscope slides for the measurement.

2.4. Catalytic Studies and Recyclability. The reaction was chosen based on the scheme reported by Chu et al.[21] The Knoevenagel reaction between 4-hydroxybenzaldehyde (1 mmol) and ethyl cyanoacetate (1 mmol) in 5 mL of ethanol, with the use of one Filter-SNF-AP (28 mg of SNF gains, 11.2 mol %) as the catalyst, was carried out in a custom-made round-bottom flask. The stirrer had no contact with the filter, and the mixture was refluxed at 80 °C for 4 h. The catalyst concentration was an estimated value based on the results (4 μmol NH_2 per mg of SNF gains) obtained, as shown in Section 2.3. The mol% was relative to the moles of 4-hydroxybenzaldehyde used. After 4 h reaction, Filter-SNF-AP was separated from the reaction mixture by forceps, rinsed with ethanol, and reused for the next Knoevenagel reaction under the same reaction conditions. The recycling process was repeated eight times. To compare the efficacy of the SNF coatings, control samples were prepared by functionalizing bare filters with APTES using the same protocol. The control was then used to catalyze Knoevenagel reaction under identical conditions.

The same reaction conditions were applied to the flow system. Four Filter-SNF-AP were packed as a column reactor to constitute the flow system. An illustration diagram for the reactor is shown in Figure 6 and is discussed in the main text. The reaction mixture was driven using a peristaltic pump (IPC 4, Ismatec) to circulate through the column at 80 °C for 4 h with a flow rate of 0.2 mL/min. Three sets of Knoevenagel reactions were carried out in equimolar quantities of 4-hydroxybenzaldehyde and ethyl cyanoacetate at 0.1, 0.2, and 0.4 M in 10 mL of ethanol, respectively. After 4 h reaction, the column was rinsed two times by 10 mL of ethanol and reused. The recycling process was repeated five times. As a comparison, control samples were used to catalyze the Knoevenagel reaction of equimolar quantities of reactants at 0.2 M under identical conditions.

In both reactors, conversions of 4-hydroxybenzaldehyde were monitored by withdrawing aliquots from the reaction mixture at the end of every cycle and analyzed by ^{1}H NMR with reference to the internal standard (duroquinone).

3. RESULTS AND DISCUSSION

3.1. SNF Coating and Characterization (Filter-SNF). Upon considering substrates that are porous will increase the surface area available for SNF coating, sintered glass filter discs were utilized for the catalytic studies. They are composed of micrometer-sized glass beads. They were expected to allow the ease of separation and recycling from the reaction mixture compared with the glass beads.

Based on the previous studies,[2,30] the structure of SNF coatings is fundamentally related to the water content in the coating chamber. Therefore, a series of experiments were done by using different combinations of relative humidity (rh) and temperature for the coating processes. Figure 1a–d shows a significant difference in the morphologies of SNFs when different methods were used to equilibrate the chamber. Needle-like nanostructures of around 3 μm heights can be observed in Figure 1b; a network of entangled SNFs can be observed in Figure 1d. Furthermore, it was confirmed by SEM that the inner part of the filters can also be coated (Figure S1).

To monitor the extent of nanostructure growth, the weight gain of the filters after the coating (Table S1) and the BET surface area were measured. An optimum coating condition was found at 27.0 ± 0.5 °C and 35 ± 5% rh, and ten filters were recorded with a weight gain >13 mg in general. A dense network of SNF without blocking the pores was also the selection criteria for the coating condition.

The efficacy of SNFs in generating the additional surface area was demonstrated using the BET results shown in Figure 1e. Filter with the highest weight gain recorded (32 mg) exhibited a BET surface area of 0.75 m^2/g. There was a 5-fold increase in the surface area compared to a bare filter with 0.14 m^2/g. Micro-sized beads after the SNF coating exhibited a BET surface area of 0.33 m^2/g. There was a 16-fold increase in

https://doi.org/10.1021/acsomega.2c06157
ACS Omega 2022, 7, 39463−39470

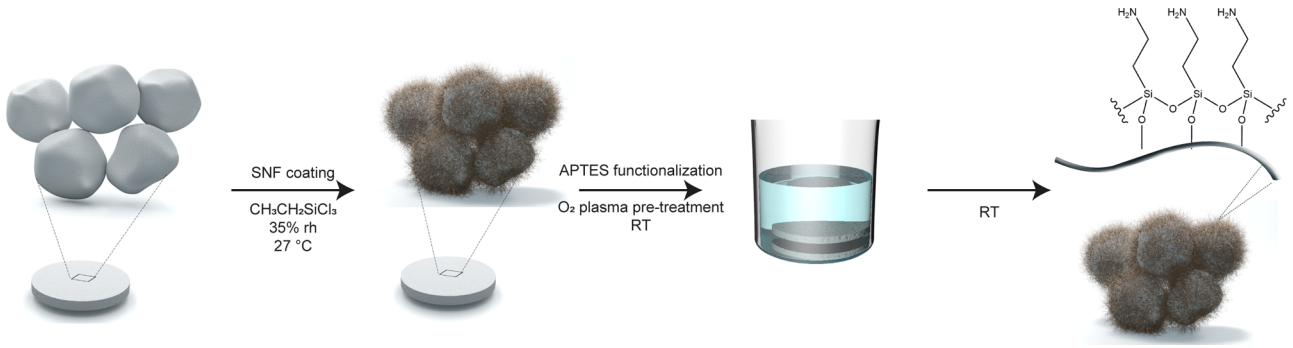

Figure 2. Illustration on the APTES functionalization of the Filter-SNF.

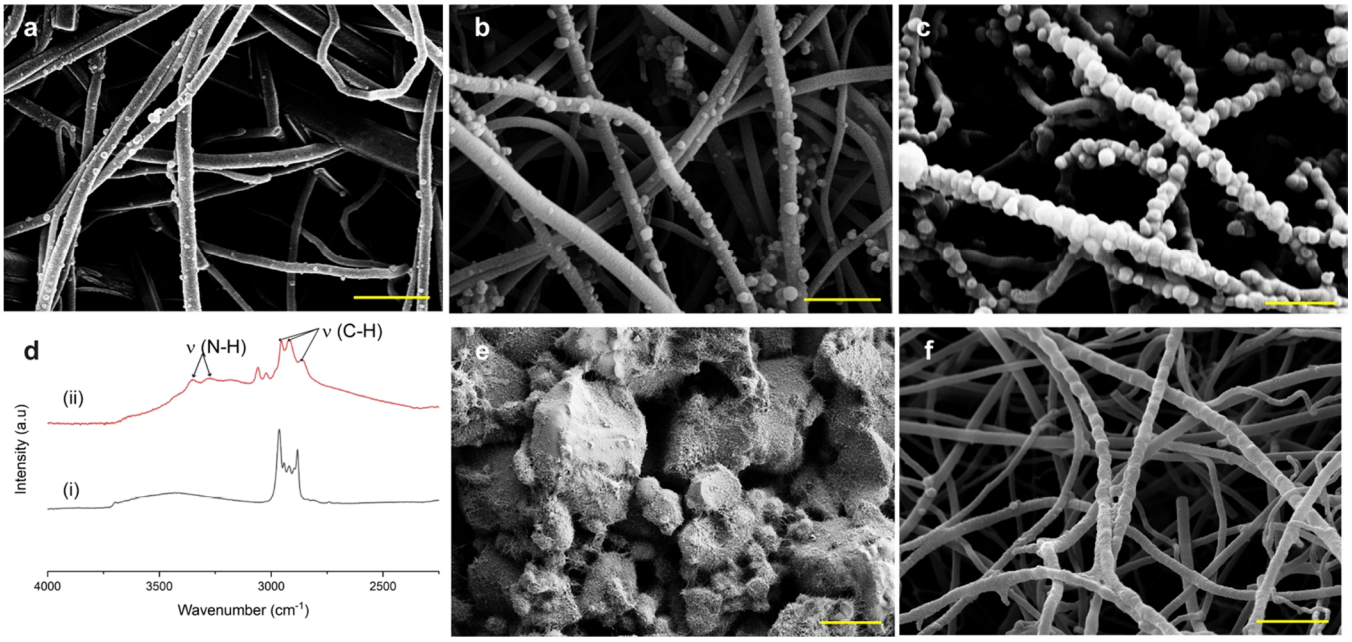

Figure 3. SEM images of SNF treated with (a) 10 mM, (b) 50 mM, and (c) 100 mM of APTES in hexane. (d) ATR-FTIR spectra of (i) SNF and (ii) SNF after being treated with APTES. (e, f) SEM images of Filter-SNF-AP after five successive cycles using the packed bed reactor. Scale bars of (a−c,f) correspond to 1 μm, and (e) corresponds to 50 μm.

the surface area compared to the bare glass beads with 0.02 m^2/g.

The influence of temperature was demonstrated when a lower temperature (23 °C) was used for the coating. With all other reaction parameters being kept the same, the BET surface area obtained was 0.49 m^2/g. This can be attributed to the lower water content in the coating chamber because of the lower temperature.

Considering that the SNF coatings were conducted in ambient conditions and the only chemical inputs were ETCS and water, the BET results demonstrated the potential of SNFs in allowing a significant expansion of surface areas of the coated substrates with a facile and environmental benign approach. The BET values herein were proof-of-concepts to demonstrate the extent of how the coatings enhance the surface area of substrates. The BET values obtained have been affected by the mass of substrates. If a suitable light weight substrate is available or only the layer of SNF coating is measured, a comparable BET value to the existing high surface area support materials[31,32] can be envisaged but required further studies.

3.2. APTES Functionalization and Characterization (Filter-SNF-AP).

To ensure consistency in the surface area generated from the SNF coating, only filters coated at the optimum conditions (27.0 ± 0.5 °C and 35 ± 5% rh) were used throughout this study.

To introduce amino moieties on Filter-SNF, functionalization was first performed by refluxing with 3-aminopropyltriethoxysilane (APTES) in toluene, given that refluxing with aminopropylalkoxysilanes is a common practice to functionalize silica-based materials with amino groups.[33] However, the approach was not ideal for Filter-SNF. An intrinsic limitation was that the nanostructures suffered from mechanical damages during reflux. A solution immersion approach was therefore adopted with reference to some of our previous studies[20,21]

Figure 2 shows the scheme to prepare an APTES-functionalized Filter-SNF (Filter-SNF-AP). As mentioned in the Experimental Section, bare filters were pre-equilibrated in the coating chamber. After the injection of ETCS, the silane penetrated and condensed on the filter surface, forming layers of surface-bound nanofilaments. To promote covalent binding of APTES with SNF, the Filter-SNF was subjected to oxygen plasma to generate more surface silanols. The filter was then

https://doi.org/10.1021/acsomega.2c06157
ACS Omega 2022, 7, 39463−39470

immersed in the reaction mixture in room temperature (RT) using a custom-made vessel, where the stirrer had no contact with the filter.

The functionalization was first conducted in toluene over different concentrations of APTES. However, it was observed that the influence of APTES concentration was more pronounced in hexane. With reference to Figure 3a−c, there was a significant increase in node growth upon higher APTES concentration. It was observed that most of the nanofilament structures collapsed after being incubated in 100 mM of APTES solution. This was not ideal as the accessibility to the amino active sites inside the filter will be reduced. Thus, 50 mM APTES solution was adopted for modifying the Filter-SNF, where the nanostructures remained unchanged.

Figure 3d shows IR spectra comparing the spectral region from 2250 to 4000 cm^{-1} obtained from the untreated and the APTES-treated SNF in their freestanding forms. This was because direct measurement on the modified filter or its grinded form have suffered from much higher signal intensity from the background substrate than the modified SNF thin layer. The spectra confirmed the presence of APTES on the SNF surfaces after the functionalization process. The characteristic band from 2850 to 3050 cm^{-1} was consistent with the previous IR spectrum of the SNF synthesized from ETCS silane precursors.[30] After APTES modification, the characteristic band was replaced by several peaks at 2860, 2920, and 2955 cm^{-1}, which were attributed to the C−H stretching of the propyl linker of APTES.[34] Furthermore, weak peaks at 3280 and 3356 cm^{-1} were identified as the N−H stretching of the amine group,[32] which provided further evidence for the modification.

The extent of APTES functionalization was determined based on a reported protocol named the acid exchange capacity method.[29] We are aware that elemental analysis and solid-state NMR[35,36] are some classical methods for quantifying functional groups on materials. However, the results from a preliminary CHNS analysis and solid-state NMR indicated that the determined APTES content was too low to be detected as reliable measurements. The problem was attributed to the fact that APTES grafting densities are intrinsically low when the whole filter substrate was measured. The variability of the acid exchange method was examined by measuring five replicates of Filter-SNF-AP. Their SNF weight gains ranged between 15 and 19 mg. The amount of accessible amino groups per mg of the SNF was determined to be 4.1 ± 0.5 μmol NH_2 with 95% confidence interval. The value, 4 μmol NH_2 per mg of SNF, will be used as a rough estimate for filters coated within the conditions 27.0 ± 0.5 °C and 35 ± 5% rh, following the same APTES functionalization protocol. The method was validated against a commercially available product, 3-aminopropyl-functionalized silica gel, as described in the Experimental Section. The amount of accessible amino groups was determined to be 1.001 ± 0.025 mmol NH_2/g with 95% confidence interval. Compared with the information provided by the supplier (∼1 mmol NH_2/g), the small variations (roughly 0.1%) demonstrated the validity of the method.

3.3. Catalytic Studies and Recyclability. The catalytic activity of the Filter-SNF-AP was examined based on the Knoevenagel condensation reaction of 4-hydroxybenzyaldehyde and ethyl cyanoacetate as the model reaction (Figure 4). The reusability of Filter-SNF-AP was evaluated over successive cycles. After the reaction, Filter-SNF-AP was rinsed and used directly for the next cycle under identical reaction conditions.

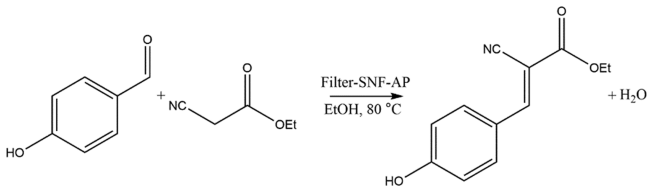

Figure 4. Knoevenagel condensation reaction of 4-hydroxybenzyaldehyde and ethyl cyanoacetate using Filter-SNF-AP as the catalyst.

A crucial issue was that the traces of the product being trapped inside the filter substrates from the previous cycles were unavoidable even with rinsing after each cycle (Figure S2). Therefore, instead of monitoring the product yield, the conversion percentages of 4-hydroxybenzyaldehyde were monitored as shown in Figure S3. This is because the actual amount of reactant was clearly known at the beginning of each cycle. The product identity was confirmed by NMR, as shown in Figure S4.

Figure 5a shows the results of the catalytic reaction using one Filter-SNF-AP (28 mg SNF gains, 11.2 mol % catalyst relative to 4-hydroxybenzyaldehyde) in the batch system. To compare the efficacy of SNF coating, a control experiment was performed using a bare filter functionalized with APTES at the same conditions. Filter-SNF-AP outperformed the control by maintaining over 80% conversion at the fifth cycle, whereas the conversion efficiency of the control sample had decreased to 22%.

When compared to other catalysts support materials, such as silica monoliths and MOFs, a significant difference of SNF coatings is the flexibility. Previous studies have demonstrated that the SNF coating can be readily applied to various materials.[1] It is envisaged that the flexibility of the SNF coating will facilitate the designs of new catalytic reactors. For examples, the SNF-based microfluidic reactor, the membrane reactor, and the flat panel photoreactor may open new opportunities.

To demonstrate the flexibility of SNF coatings in enabling the design of the catalytic reactor, Figure 6 presents the design of a packed bed reactor by packing several Filter-SNF-AP into a column. The stream of the reagent was circulated within the system to provide sufficient residence time between the catalyst and the reagent. Inert PTFE rings were placed in between filters (Figure 6b) to serve two purposes. First, filters were fixed in their position to minimize mechanical abrasions. Second, the rings were tightly pressed against the column wall to force the reagents to flow through the filters. In addition, the stream of the reagent was directly delivered to the filters at a flow rate of 0.2 mL/min through a tube.

Figure 5b shows the results of the catalytic reaction using four Filter-SNF-AP in the packed bed reactor. The size of the system has doubled compared to the batch reactor, so that there is enough volume to maintain the circulation. Based on the studies performed on the batch reactor, the experiment was first conducted at the same concentration of the reagent (0.2 M). There was no significant difference over the conversion efficiency when compared to the result of the batch reactor. Around 80% conversion was maintained for five cycles. The system was further tested by varying the concentrations of the reagent. At 0.1 M concentration of the reagent, over 90% conversion was maintained throughout five successive cycles. The efficacy of having the functionalized SNF coatings on the substrate was more prominent in the flow system when

https://doi.org/10.1021/acsomega.2c06157
ACS Omega 2022, 7, 39463−39470

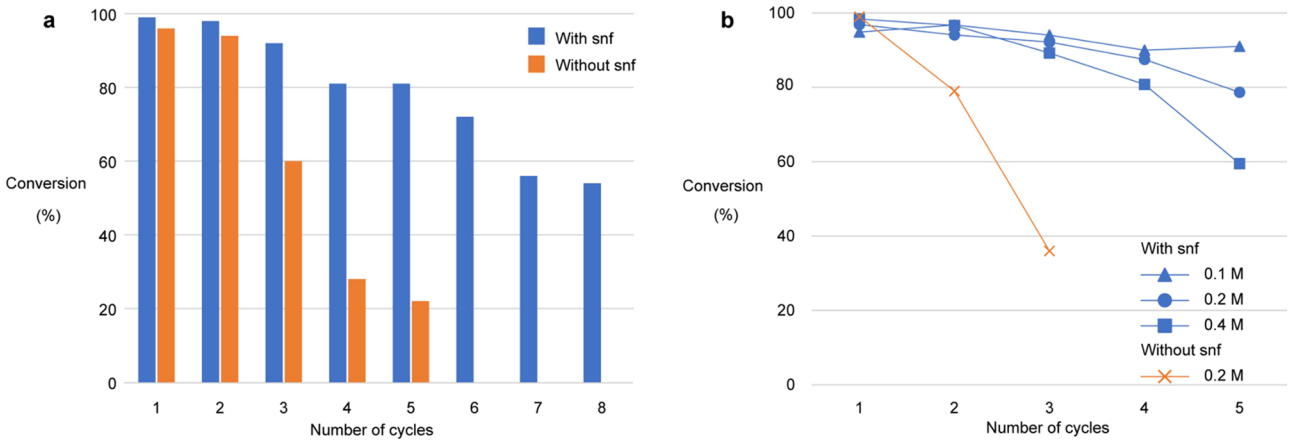

Figure 5. Comparison on the conversion of 4-hydroxybenzyaldehyde (0.2 M) catalyzed by Filter-SNF-AP and the control sample (a) using the batch reactor eight cycles and (b) using the packed bed reactor five cycles. The performance of Filter-SNF-AP was also tested against varying concentrations of reactants (0.1 and 0.4 M) using the packed bed reactor.

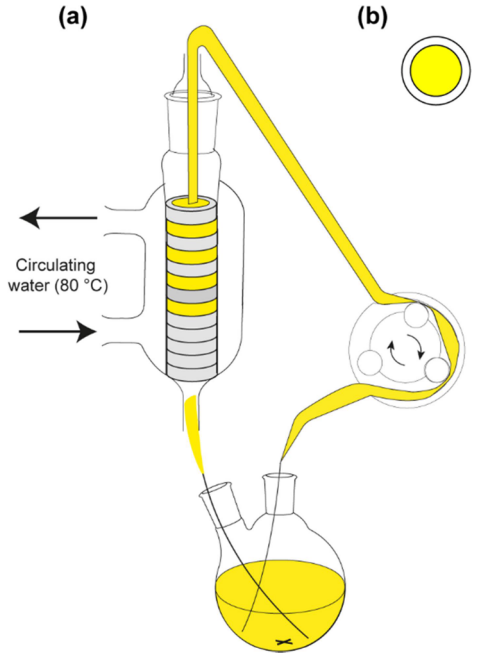

Figure 6. (a) Illustration diagram of the packed bed reactor. (b) Top view of the PTFE ring placed between filters.

compared with the control. The conversion efficiency of the control samples has decreased drastically at the third cycle.

Filter-SNF-AP after five successive runs in the packed bed reactor was examined by SEM (Figures 3e,f). Most of the SNF structures remained intact, except some at the outer surface were abraded. Given that mechanical stability is a profound challenge to coating materials in general, the utilization of supported catalysts based on catalytic coatings is not practicable with stirring in a batch reactor. Herein, the batch reactor was specifically designed to separate the catalyst with the magnetic stirrer. However, the addition of Filter-SNF-AP was still not possible because of abrasion between filters. The packed bed reactor established in this study has demonstrated its utility to overcome the challenge. The reactor has facilitated the use of SNF-supported catalysts, where mechanical interventions related to stirring and separation of catalysts between reaction cycles were avoided.

Even though significant mechanical deterioration of the SNF structures was not observed, a decline in the conversion efficiency of Filter-SNF-AP upon increasing reaction cycles was noticed in both batch and flow systems (Figure 5). The decline in performance also occurred in those uncoated substrates. A plausible reason could be attributed to the hydrolytic degradation of APTES under basic conditions and high temperature.[37,38] The observable morphology changes between Figures 3b,e have supported this proposition. Future studies regarding the types of catalytic reactions and the grafted catalysts would be of value for improving the catalytic efficiency of SNF-supported catalysts.

The results from the catalytic studies have demonstrated the successful establishment of a packed bed catalytic reactor for the use of SNF-supported organocatalysts. The facile preparation of the reactor by packing several organically functionalized, SNF-coated filters has demonstrated the versatility of SNF coatings as catalyst supports. The catalytic SNF coatings were transformed into individual catalytic composite units and were less prone to mechanical damages. The packed bed reactor has also shown adaptability to a system scale-up. The advantage of the SNF coatings was clearly demonstrated when comparing the catalytic efficiency with the uncoated counterparts in both batch and flow systems. The enhancement in catalytic performance could be attributed to the larger surface area provided by the SNF, where higher catalyst loadings and accessibility to the active sites were promoted.

Recent research interest on the designs of catalytic systems for targeted applications has gradually shifted from the syntheses of novel catalysts to the architectural designs of known catalytic materials.[39] For example, the preparation of catalytic active materials such as metal oxides and zeolites has extended from bulk forms into thin films and coatings. This has allowed the same catalytic material to carry out the targeted application in a different format, where new properties and applications were discovered. For instance, the occurrence of microreactor technology and flow chemistry. In this study, the incorporation of catalytic SNF coatings in a flow system was demonstrated. We anticipate that the SNF coatings will be attractive catalyst support materials amid the ongoing research and development of catalytic active thin films and coatings. Furthermore, we anticipate that the flexibility in the Filter-

https://doi.org/10.1021/acsomega.2c06157
ACS Omega 2022, 7, 39463−39470

SNF-AP catalytic units and the packed bed column will allow interesting applications in tandem catalysis.[40,41]

4. CONCLUSIONS

A series of experiments were done to optimize the extent of SNF growth on glass filters and glass beads. The extent on how SNF coatings enhance the surface area of substrates was quantified by BET measurements. The BET surface area of a bare filter substrate has increased by 5-folds after the SNF coating and 16-folds for bare glass beads substrates. Notably, when the temperature of the coating chamber increased by 5 °C, the BET value increased from 0.49 to 0.75 m^2/g with the same amount of ETCS inputs. Given the synthesis of these SNF coatings were conducted in ambient conditions and the only chemical inputs required were ETCS and water, these suggested the potential of SNFs to offer a facile and environmentally benign approach for the preparation of high surface area support materials.

APTES was used to modify the SNF-coated substrates via a solution immersion approach at room temperature. The comparisons of the catalytic performance between Filter-SNF-AP and the functionalized uncoated filters in both batch and flow systems have clearly demonstrated the advantage of SNFs in enhancing the catalytic efficiency of the substrates. The fact that SNFs are synthesized under ambient conditions provides an environmentally friendly alternative to the existing catalyst supports.

To the best of our knowledge, this is the first report of using organically functionalized, SNF-coated composites as a packed bed catalytic reactor. The flexibility of SNF coatings has enabled the facile preparation of a packed bed reactor and a scalable catalytic system. It is anticipated that the packed bed system established in this study will support the development of various SNF-supported catalytic materials and may find applications in tandem catalysis.

■ ASSOCIATED CONTENT

Supporting Information

The Supporting Information is available free of charge at https://pubs.acs.org/doi/10.1021/acsomega.2c06157.

SEM images of Filter-SNF, net weight gain of filters after SNF coating under different coating conditions; photo image of Filter-SNF-AP after reaction; and ^{1}H NMR spectra of the Knoevenagel reaction (PDF)

■ AUTHOR INFORMATION

Corresponding Author

Stefan Seeger − *Department of Chemistry, University of Zurich, CH-8057 Zurich, Switzerland;* orcid.org/0000-0003-2892-7468; Email: sseeger@chem.uzh.ch

Authors

Yuen-Yee Lau − *Department of Chemistry, University of Zurich, CH-8057 Zurich, Switzerland*

Kangwei Chen − *Department of Chemistry, University of Zurich, CH-8057 Zurich, Switzerland;* orcid.org/0000-0002-2977-2464

Shanqiu Liu − *Department of Chemistry, University of Zurich, CH-8057 Zurich, Switzerland;* Present Address: College of Materials Science & Engineering, Zhejiang University of Technology, Hangzhou 310014, P. R. China; orcid.org/0000-0002-6816-7507

Lukas Reith − *Department of Chemistry, University of Zurich, CH-8057 Zurich, Switzerland;* orcid.org/0000-0003-4874-1476

Complete contact information is available at: https://pubs.acs.org/10.1021/acsomega.2c06157

Notes

The authors declare no competing financial interest.

■ ACKNOWLEDGMENTS

The authors would like to acknowledge Roland Zehnder at the mechanical workshop, the glass workshop, and the Center for Microscopy and Image Analysis of the University of Zurich for their support and for use of their facilities. We also thank our colleagues, especially Dr. Georg Artus, Davide Bottone, and Alessandro De Crema for the valuable discussions.

■ REFERENCES

(1) Artus, G. R. J.; Jung, S.; Zimmermann, J.; Gautschi, H.-P.; Marquardt, K.; Seeger, S. Silicone Nanofilaments and Their Application as Superhydrophobic Coatings. *Adv. Mater.* **2006**, *18*, 2758−2762.

(2) Artus, G. R. J.; Olveira, S.; Patra, D.; Seeger, S. Directed In Situ Shaping of Complex Nano- and Microstructures during Chemical Synthesis. *Macromol. Rapid Commun.* **2017**, *38*, No. 1600558.

(3) Zimmermann, J.; Artus, G. R. J.; Seeger, S. Long term studies on the chemical stability of a superhydrophobic silicone nanofilament coating. *Appl. Surf. Sci.* **2007**, *253*, 5972−5979.

(4) Zhang, J.; Seeger, S. Silica/Silicone Nanofilament Hybrid Coatings with Almost Perfect Superhydrophobicity. *ChemPhysChem* **2013**, *14*, 1646−1651.

(5) Liu, S.; Zhang, X.; Seeger, S. Solvent-Free Fabrication of Flexible and Robust Superhydrophobic Composite Films with Hierarchical Micro/Nanostructures and Durable Self-Cleaning Functionality. *ACS Appl. Mater. Interfaces* **2019**, *11*, 44691−44699.

(6) Ouyang, S.; Wang, T.; Jia, X.; Chen, Y.; Yao, J.; Wang, S. Self-indicating and recyclable superhydrophobic membranes for effective oil/water separation in harsh conditions. *Mater. Des.* **2016**, *96*, 357−363.

(7) Dong, T.; Li, Q.; Nie, K.; Jiang, W.; Li, S.; Hu, X.; Han, G. Facile Fabrication of Marine Algae-Based Robust Superhydrophobic Sponges for Efficient Oil Removal from Water. *ACS Omega* **2020**, *5*, 21745−21752.

(8) Yin, H.; Moghaddam, M. S.; Tuominen, M.; Eriksson, M.; Järn, M.; Dėdinaitė, A.; Wålinder, M.; Swerin, A. Superamphiphobic plastrons on wood and their effects on liquid repellence. *Mater. Des.* **2020**, *195*, No. 108974.

(9) Laroche, A.; Ritzen, L.; Guillén, J. A. M.; Vercillo, V.; D'Acunzi, M.; Aghili, A. S.; Hussong, J.; Vollmer, D.; Bonaccurso, E. Durability of Superamphiphobic Polyester Fabrics in Simulated Aerodynamic Icing Conditions. *Coatings* **2020**, *10*, 1058.

(10) Saddiqi, N.-U.-H.; Patra, D.; Seeger, S. Room-Temperature Synthesis of Germanium Oxide Nanofilaments and Their Potential Use as Luminescent Self-Cleaning Surfaces. *ChemPhysChem* **2019**, *20*, 538−544.

(11) Hua, Z.; Yang, J.; Wang, T.; Liu, G.; Zhang, G. Transparent Surface with Reversibly Switchable Wettability between Superhydrophobicity and Superhydrophilicity. *Langmuir* **2013**, *29*, 10307−10312.

(12) Shen, Y.; Li, D.; Wang, L.; Zhou, Y.; Liu, F.; Wu, H.; Deng, B.; Liu, Q. Superelastic Polyimide Nanofiber-Based Aerogels Modified with Silicone Nanofilaments for Ultrafast Oil/Water Separation. *ACS Appl. Mater. Interfaces* **2021**, *13*, 20489−20500.

(13) Kasapgil, E.; Badv, M.; Cantú, C. A.; Rahmani, S.; Erbil, H. Y.; Sakir, I. A.; Weitz, J. I.; Hosseini-Doust, Z.; Didar, T. F. Polysiloxane Nanofilaments Infused with Silicone Oil Prevent Bacterial Adhesion

and Suppress Thrombosis on Intranasal Splints. *ACS Biomater. Sci. Eng.* **2021**, *7*, 541−552.
(14) Zhang, J.; Seeger, S. Polyester Materials with Superwetting Silicone Nanofilaments for Oil/Water Separation and Selective Oil Absorption. *Adv. Funct. Mater.* **2011**, *21*, 4699−4704.
(15) Duan, B.; Gao, H.; He, M.; Zhang, L. Hydrophobic Modification on Surface of Chitin Sponges for Highly Effective Separation of Oil. *ACS Appl. Mater. Interfaces* **2014**, *6*, 19933−19942.
(16) Meseck, G. R. *Silicone Nanofilaments as High Surface Area Support for Catalysts*; Ph.D. Dissertation; University of Zurich: Switzerland, 2014
(17) Meseck, G. R.; Kontic, R.; Patzke, G. R.; Seeger, S. Photocatalytic Composites of Silicone Nanofilaments and TiO2 Nanoparticles. *Adv. Funct. Mater.* **2012**, *22*, 4433−4438.
(18) Abbott, D. F.; Meier, M.; Meseck, G. R.; Fabbri, E.; Seeger, S.; Schmidt, T. J. Silicone Nanofilament-Supported Mixed Nickel-Metal Oxides for Alkaline Water Electrolysis. *J. Electrochem. Soc.* **2017**, *164*, F203−F208.
(19) Li, J.; Li, L.; Du, X.; Feng, W.; Welle, A.; Trapp, O.; Grunze, M.; Hirtz, M.; Levkin, P. A. Reactive Superhydrophobic Surface and Its Photoinduced Disulfide-ene and Thiol-ene (Bio)functionalization. *Nano Lett.* **2015**, *15*, 675−681.
(20) Zimmermann, J.; Rabe, M.; Verdes, D.; Seeger, S. Functionalized Silicone Nanofilaments: A Novel Material for Selective Protein Enrichment. *Langmuir* **2007**, *24*, 1053−1057.
(21) Chu, Z.; Seeger, S. Multifunctional Hybrid Porous Micro-/Nanocomposite Materials. *Adv. Mater.* **2015**, *27*, 7775−7781.
(22) Luis, S. V.; Garcia-Verdugo, E. Flow Chemistry: Integrated Approaches for Practical Applications, Green Chemistry Series No. 62. *R. Soc. Chem.* **2020**, 1−49.
(23) Colella, M.; Carlucci, C.; Luisi, R. Supported Catalysts for Continuous Flow Synthesis. *Top. Curr. Chem.* **2018**, *376*, 46.
(24) Yan, Y.; Miao, J.; Yang, Z.; Xiao, F.-X.; Yang, H. B.; Liu, B.; Yang, Y. Carbon nanotube catalysts: recent advances in synthesis, characterization and applications. *Chem. Soc. Rev.* **2015**, *44*, 3295−3346.
(25) Lu, W.; He, T.; Xu, B.; He, X.; Adidharma, H.; Radosz, M.; Gasem, K.; Fan, M. Progress in catalytic synthesis of advanced carbon nanofibers. *J. Mater. Chem. A* **2017**, *5*, 13863−13881.
(26) Cai, Z.; Liu, B.; Zou, X.; Cheng, H.-M. Chemical Vapor Deposition Growth and Applications of Two-Dimensional Materials and Their Heterostructures. *Chem. Rev.* **2018**, *118*, 6091−6133.
(27) Zimmermann, J.; Reifler, F. A.; Fortunato, G.; Gerhardt, L.-C.; Seeger, S. A Simple, One-Step Approach to Durable and Robust Superhydrophobic Textiles. *Adv. Funct. Mater.* **2008**, *18*, 3662−3669.
(28) Almkhelfe, H.; Carpena-Núñez, J.; Back, T. C.; Amama, P. B. Gaseous product mixture from Fischer−Tropsch synthesis as an efficient carbon feedstock for low temperature CVD growth of carbon nanotube carpets. *Nanoscale* **2016**, *8*, 13476−13487.
(29) Li, G.; Xiao, J.; Zhang, W. Knoevenagel condensation catalyzed by a tertiary-amine functionalized polyacrylonitrile fiber. *Green Chem.* **2011**, *13*, 1828−1836.
(30) Stojanovic, A.; Olveira, S.; Fischer, M.; Seeger, S. Polysiloxane Nanotubes. *Chem. Mater.* **2013**, *25*, 2787−2792.
(31) Parlett, C. M. A.; Wilson, K.; Lee, A. F. Hierarchical porous materials: catalytic applications. *Chem. Soc. Rev.* **2013**, *42*, 3876−3893.
(32) Perego, C.; Millini, R. Porous materials in catalysis: challenges for mesoporous materials. *Chem. Soc. Rev.* **2013**, *42*, 3956−3976.
(33) Ritter, H.; Nieminen, M.; Karppinen, M.; Brühwiler, D. A comparative study of the functionalization of mesoporous silica MCM-41 by deposition of 3-aminopropyltrimethoxysilane from toluene and from the vapor phase. *Microporous Mesoporous Mater.* **2009**, *121*, 79−83.
(34) Turke, K.; Meinusch, R.; Cop, P.; da Costa, E. P.; Brand, R. D.; Henss, A.; Schreiner, P. R.; Smarsly, B. M. Amine-Functionalized Nanoporous Silica Monoliths for Heterogeneous Catalysis of the Knoevenagel Condensation in Flow. *ACS Omega* **2021**, *6*, 425−437.
(35) Huh, S.; Wiench, J. W.; Yoo, J.-C.; Pruski, M.; Lin, V. S.-Y. Organic Functionalization and Morphology Control of Mesoporous Silicas via a Co-Condensation Synthesis Method. *Chem. Mater.* **2003**, *15*, 4247−4256.
(36) Davidowski, S. K.; Holland, G. P. Solid-State NMR Characterization of Mixed Phosphonic Acid Ligand Binding and Organization on Silica Nanoparticles. *Langmuir* **2016**, *32*, 3253−3261.
(37) Smith, E. A.; Chen, W. How To Prevent the Loss of Surface Functionality Derived from Aminosilanes. *Langmuir* **2008**, *24*, 12405−12409.
(38) Kunc, F.; Balhara, V.; Brinkmann, A.; Sun, Y.; Leek, D. M.; Johnston, L. J. Quantification and Stability Determination of Surface Amine Groups on Silica Nanoparticles Using Solution NMR. *Anal. Chem.* **2018**, *90*, 13322−13330.
(39) Mehla, S.; Das, J.; Jampaiah, D.; Periasamy, S.; Nafady, A.; Bhargava, S. K. Recent advances in preparation methods for catalytic thin films and coatings. *Catal. Sci. Technol.* **2019**, *9*, 3582−3602.
(40) Denard, C. A.; Hartwig, J. F.; Zhao, H. Multistep One-Pot Reactions Combining Biocatalysts and Chemical Catalysts for Asymmetric Synthesis. *ACS Catal.* **2013**, *3*, 2856−2864.
(41) Wasilke, J.-C.; Obrey, S. J.; Baker, R. T.; Bazan, G. C. Concurrent Tandem Catalysis. *Chem. Rev.* **2005**, *105*, 1001−1020.

https://doi.org/10.1021/acsomega.2c06157
ACS Omega 2022, 7, 39463−39470